Supporting information

Cell microenvironment pH sensing in 3D microgels using fluorescent carbon dots

Anil Chandra [a] and Neetu Singh [a,b*]

[a] Centre for Biomedical Engineering, Indian Institute of Technology Delhi, Hauz Khas, New Delhi-110016, India

[b] Department of Biomedical Engineering, All India Institute of Medical Sciences, Ansari Nagar, New Delhi-110029, India

*E-mail: sneetu@iitd.ac.in Fax: + 91-11-26582037 Tel: + 91-11-2659-1422

Number of pages: 14

Number of figures: 22

Characterization

A. **Absorbance spectroscopy:** The absorbance spectra of carbon dot solution was collected using Take3 BioTek synergy H1 Multimode reader. The absorbance showed typical peaks for π-π* and n-π* transition at 254 and 30 nm respectively.

B. **Fluorescence spectroscopy:** Fluorescence spectrum of carbon dots dispersed in deionized water were taken against different excitation wavelengths starting from 365 nm to 500nm.

C. **Transmission electron microscopy (TEM):** Size of carbon dots was estimated by transmission electron microscopy. Thoroughly cleaned dispersion of carbon dots in deionized water were drop casted on 200 mesh carbon coated copper grid and dried in vacuum desiccator. Prepared grids were analyzed on T20 Tecnai electron microscope with electron acceleration voltage of 200 kV.

D. **Zeta Potential estimation** Zeta potential of carbon dots dispersed in phosphate buffer saline maintained at different pH values was measured by Malvern Nano ZS90 particle size. The pH of the PBS was adjusted by addition of HCl and NaOH.

E. **Scanning electron microscopy:** Size of PEG hydrogel formed were assessed using scanning electron microscopy. The microgels suspended in deionized water were drop casted on a glass piece of size 1cm x 1cm. Water on the glass was carefully removed from the edge using tissue paper leaving microgels on the surface of glass. The microgels were dried either at room temperature in a desiccator or by freeze drying. Freeze drying was done to observe porous structure of the microgel, which otherwise vanished under normal drying. The dried microgels were sputtered with gold and analyzed by SEM.

F. **Quantum yield measurement**

Quantum yield of carbon dots for blue emission was estimated by using Quinine hemisulphate in 0.1 M H_2SO_4 (Φ= 0.54) as reference fluorophore. Quantum yield of carbon dots for green emission was estimated by taking fluorescein in 0.1 M NaOH (Φ= 0.79) as reference fluorophore. The absorbance of all dispersions in deionised water was kept below 0.1 to avoid problem of reabsorption. The following equation is used to calculate the quantum yield

$$\boldsymbol{\Phi_f^i = \frac{F^i f^s n_i^2}{F^s f^i n_s^2} \Phi_f^s}$$

Where,

$\boldsymbol{\Phi_f^i}$ and $\boldsymbol{\Phi_f^s}$: Quantum yield of the sample and standard

$\boldsymbol{F^i}$ and $\boldsymbol{F^s}$: Integrated fluorescence intensity (area under the curve) of sample and standard

$\boldsymbol{f^i}$ and $\boldsymbol{f^s}$: Absorption of sample and standard

$\boldsymbol{n_i^2}$ and $\boldsymbol{n_s^2}$: Refractive indices of sample and standard

Microgel cell culture under paraffin oil

After formation of microgels containing cells and carbon dots, they were washed thrice with phosphate buffer saline to unpolymerized monomer, photoinitiator and loosely bound carbon dots. Microgels were then soaked in phenol red free DMEM media for 5 minutes and then transferred to glass petri plate containing light liquid paraffin. The petriplate containing microgels submerged in oil were then placed at 37 °C in CO_2 incubator. The microgels were imaged at regular intervals using fluorescence microscopy to observe the increase in fluorescence corresponding to cell growth over time.

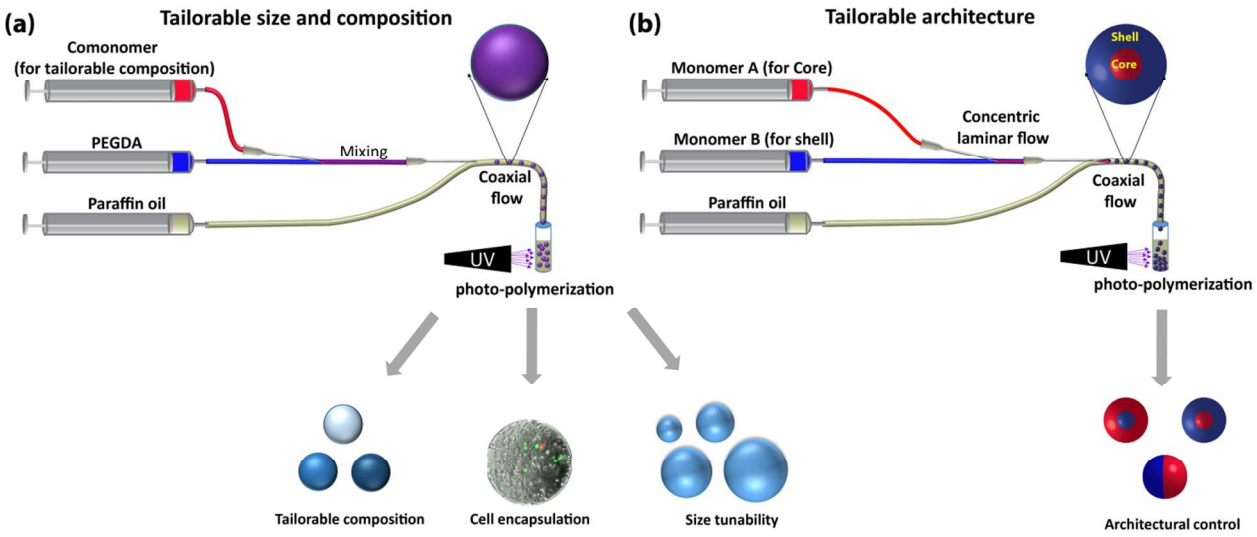

Figure S1. Schematic showing system for microgel formation (a) Arrangement for microgel generation with tailorable size and composition. (b) Arrangement for generation of microgels with controlled architecture.

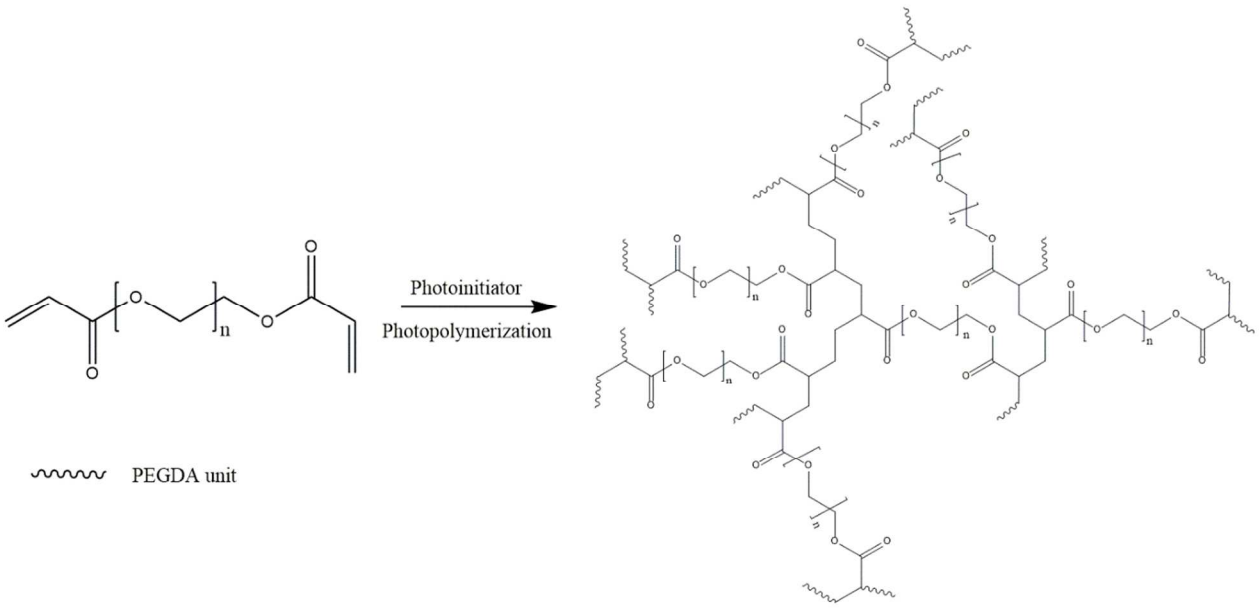

Figure S2: Schematic showing chemical structure of PEG hydrogel network after photo-polymerization of PEGDA.

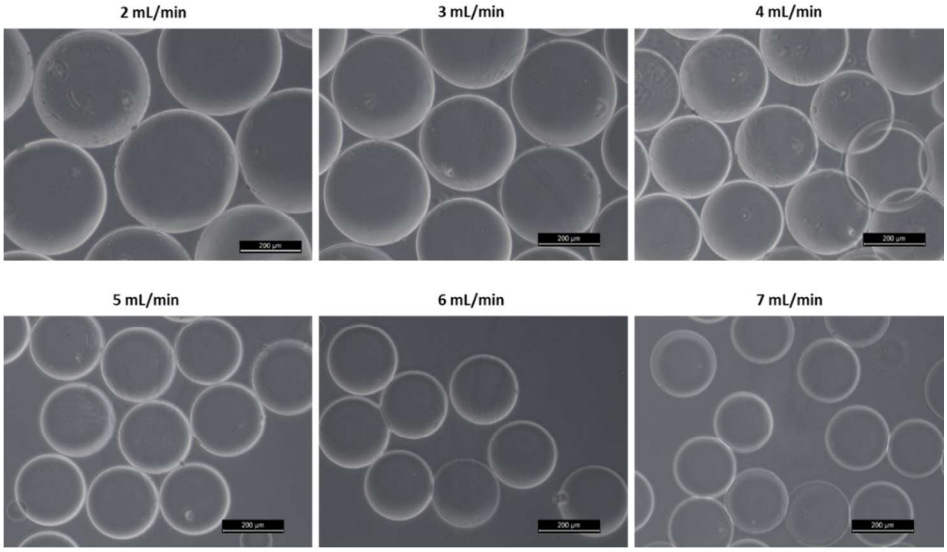

Figure S3. Bright field microscopy images showing control over size of microdroplet being produced. Microgel size decreases with increase in continuous phase (paraffin oil) velocity

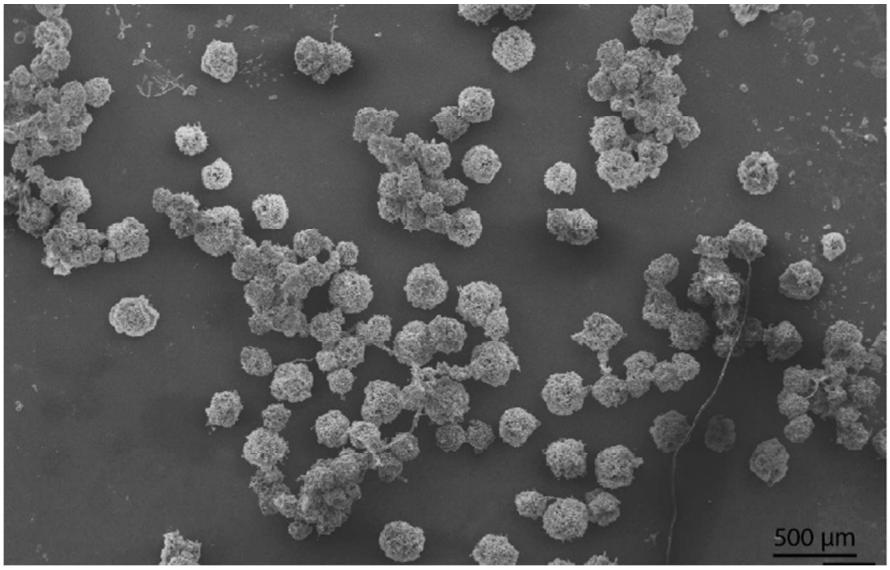

Figure S4. Scanning electron microscopy image showing monodispersed porous microgels.

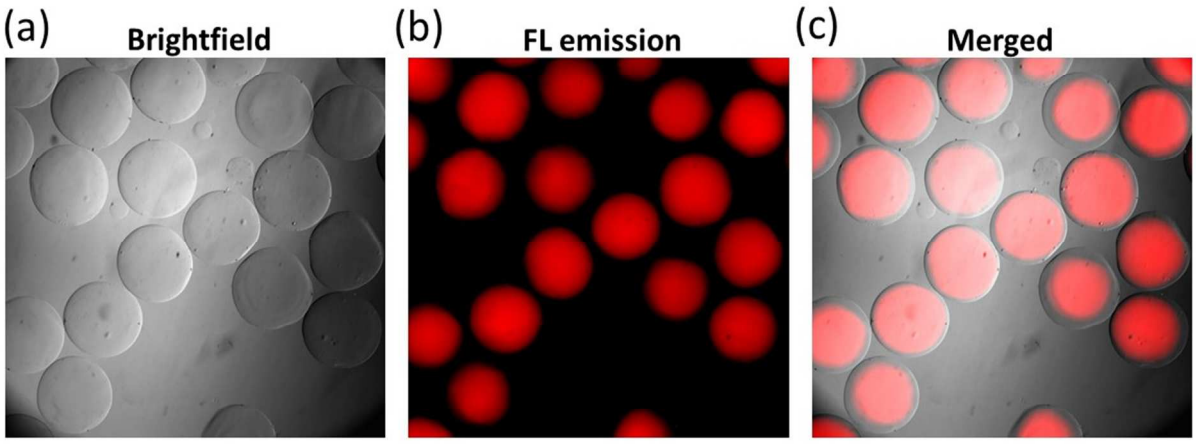

Figure S5. (a) Bright field image of microgels (b) Image showing fluorescence (FL) emission from microgels after conjugation of rhodamine 6G with acrylic acid in the core (c) Merged image indicating presence of fluorescence from the core due to Rhodamine 6G and its absence indicated by a clear and transparent outer shell (only PEG)

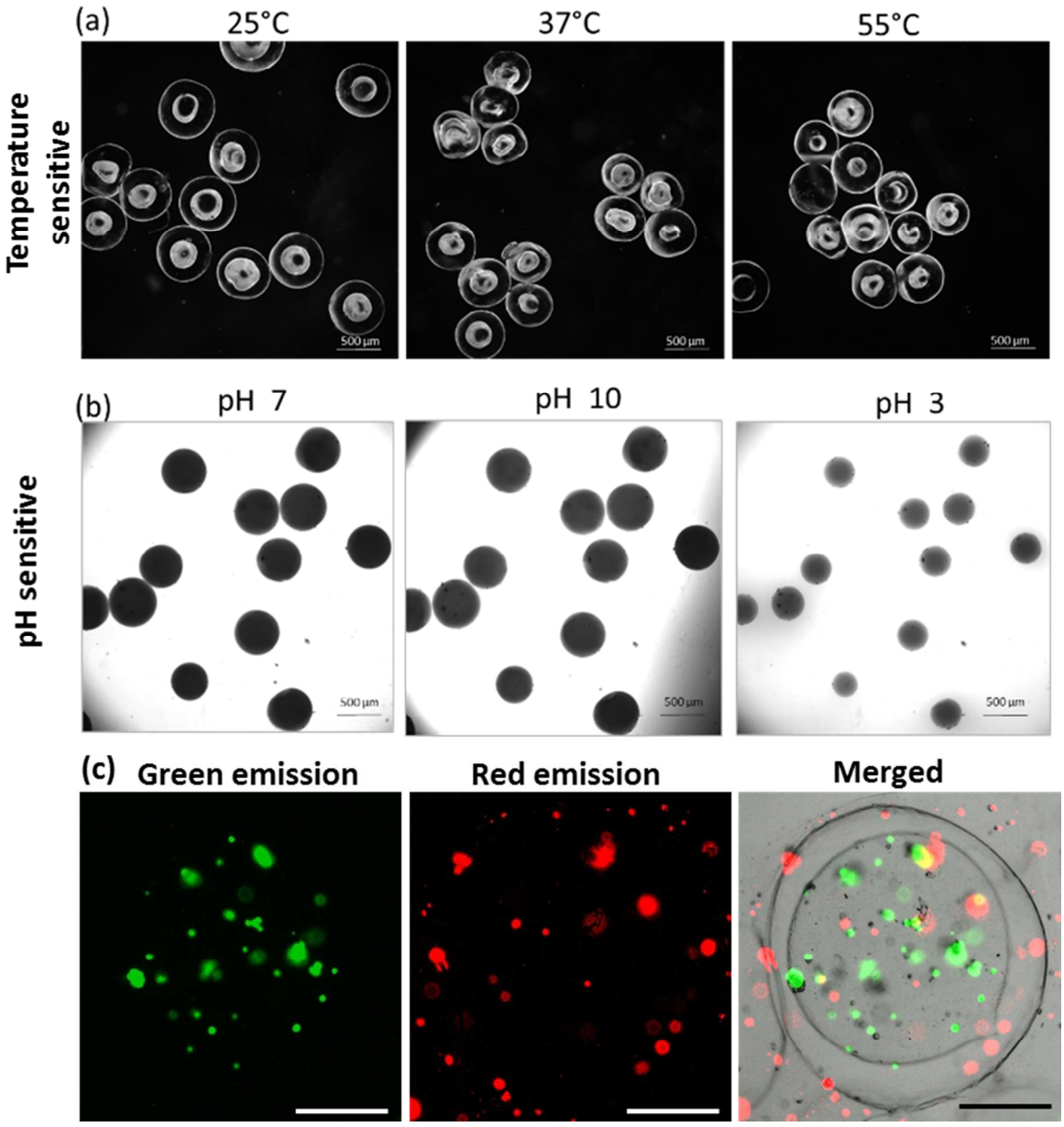

Figure S6. (a) Dark field image showing temperature sensitive microgels with *p*(NIPAm-co-PEGDA) at the core along with PEG shell showing decrease in volume with increase in temperature. (b) Brightfield image showing pH responsive microgels containing acrylic acid as co-monomers in the core along with only PEG shell showing shrinkage at acidic pH. (c) Fluorescence microscopy image showing red cells in the shell and green cells in the core, showing example of controlled architecture in co-culture applications.

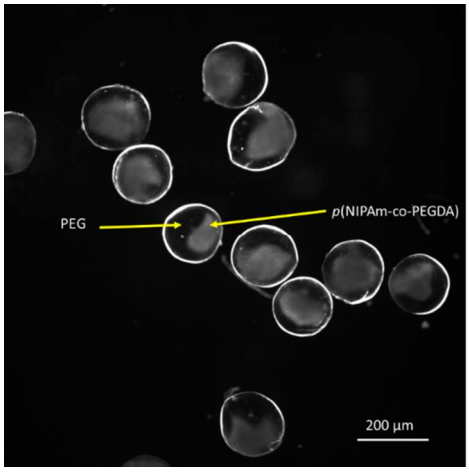

Figure S7. Janus microgels having halves made from PEGDA (transparent) and *p*(NIPAm-co-PEGDA) (opaque)

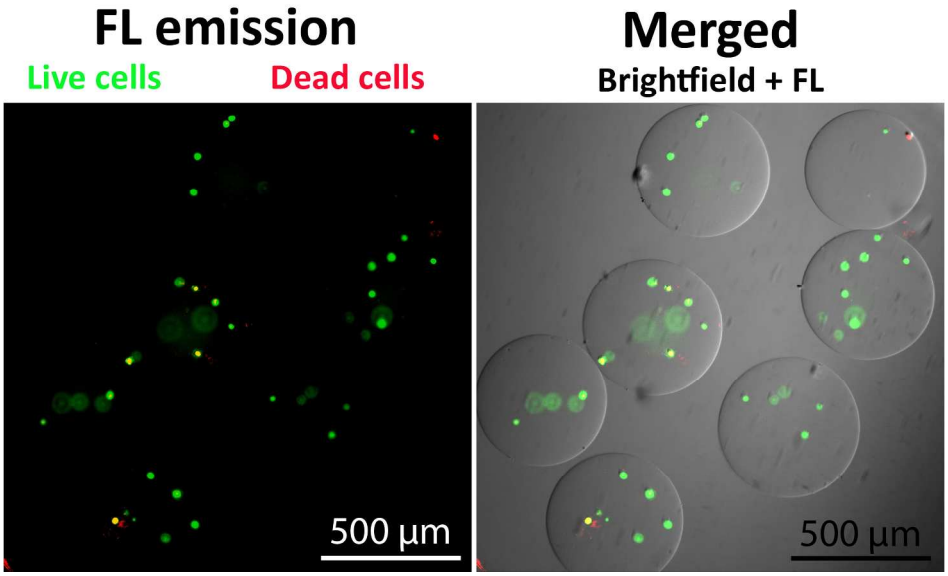

Figure S8. Live dead assay for NIH-3T3 cells encapsulated in microgel after 12 days.

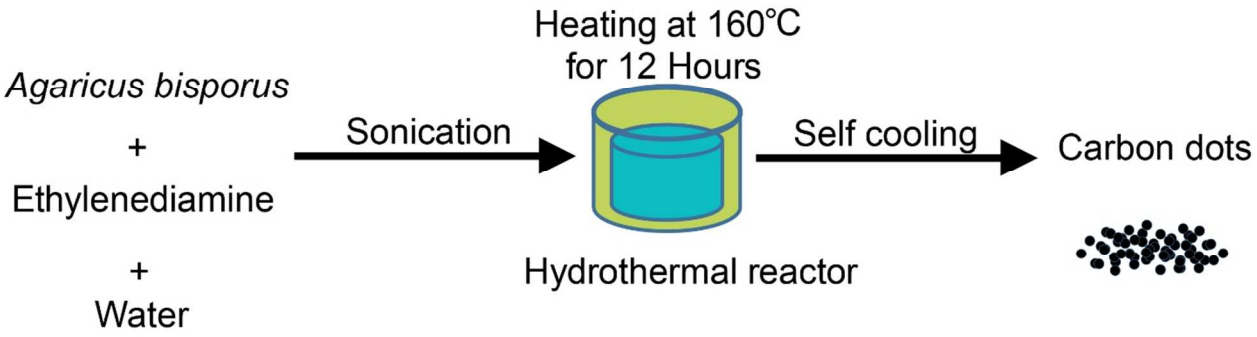

Figure S9. Synthesis of carbon dots using hydrothermal reaction.

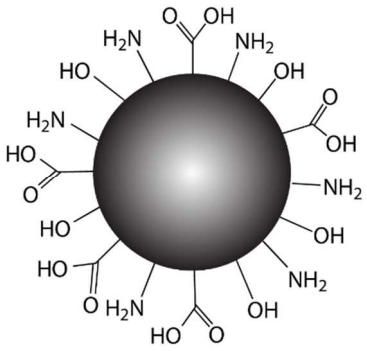

Figure S10: Chemical structure of carbon dots showing functional groups present on its surface.

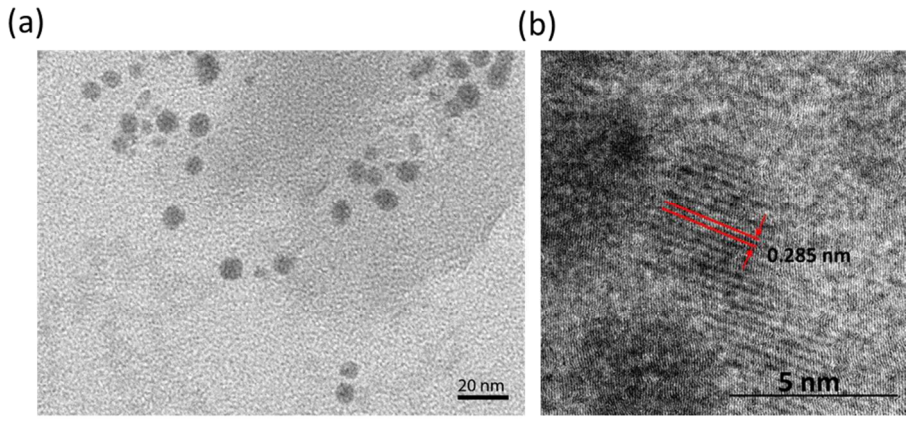

Figure S11. (a) Transmission electron microscopy of carbon dots. Average diameter is 5.18±1.3 nm. (b) HRTEM image of carbon dot showing lattice spacing of 0.285 nm indicating presence of 002 plane of graphitic carbon.

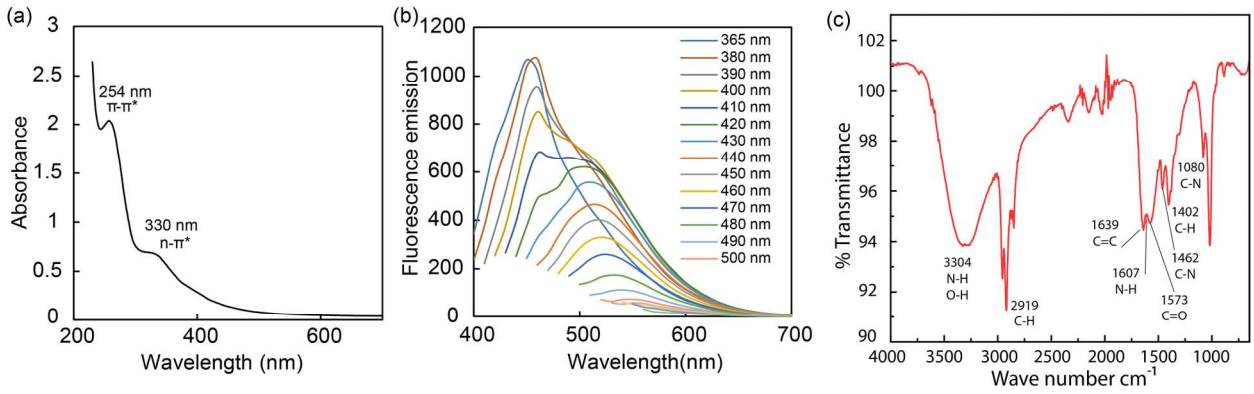

Figure S12. (a) Absorbance spectra showing signature peaks for carbon dots at 254 nm indicating π-π* transition and 330 nm due to n-π* transition. (b) Fluorescence spectra of carbon dots using different excitation wavelengths showing excitation dependent emission red shift. (c) FTIR spectrum of carbon dots showing presence of various functional groups.

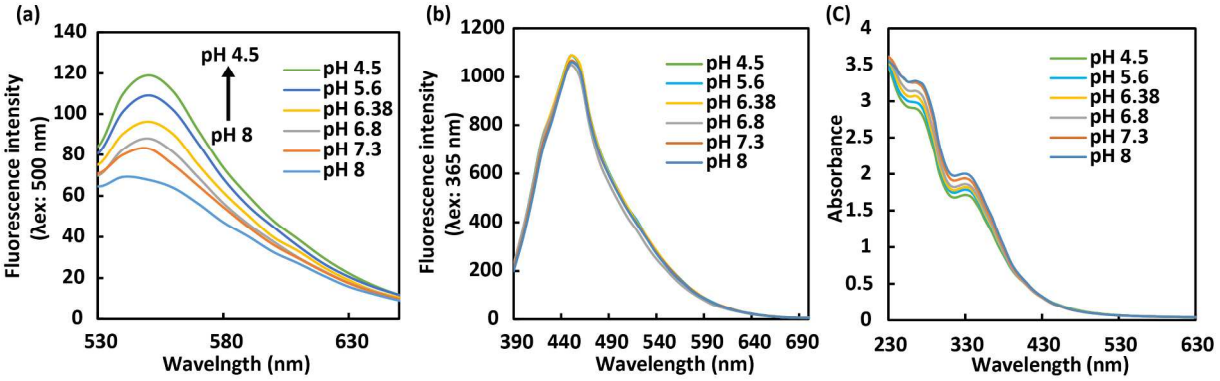

Figure S13. (a) Fluorescence spectra of carbon dots at different pH values when excited at 500 nm. The fluorescence increases with decrease in pH values. (b) Fluorescence spectra of carbon dots at different pH values when excited at 365 nm. There is no change in emission intensity. (c) Absorbance spectra of carbon dots against different pH values.

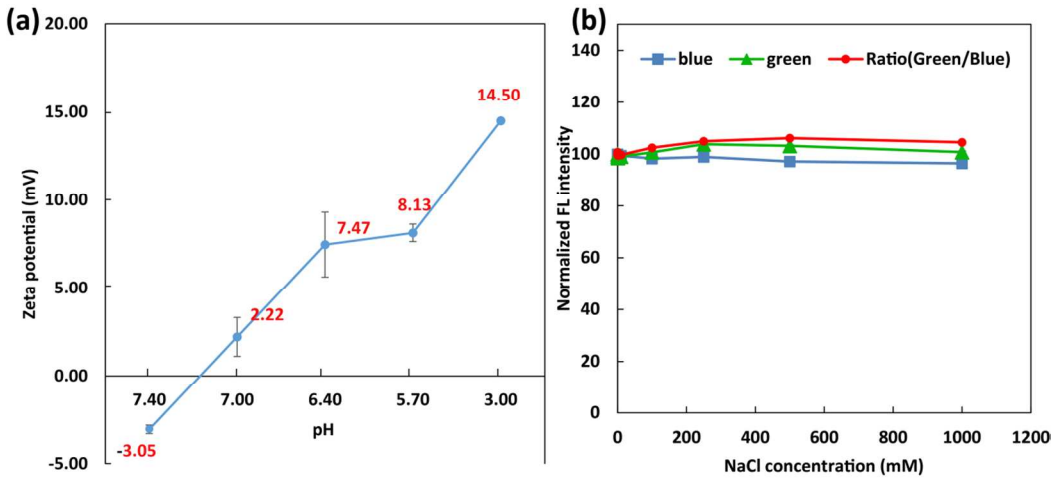

Figure S14: (a) Plot showing relationship between pH and zeta potential. (b) Plot showing effect of ionic strength on green, blue and (green/blue) emission intensity of carbon dots.

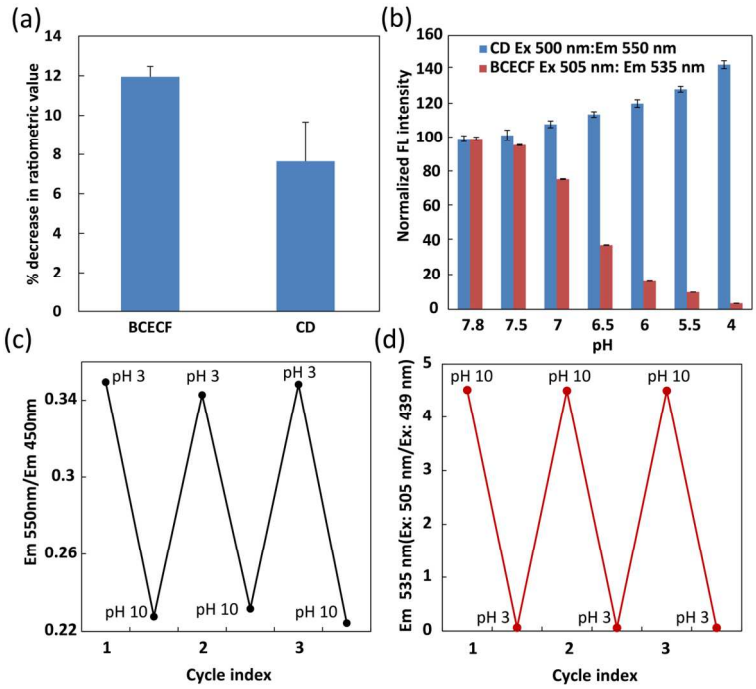

Figure S15: (a) Relative change in fluorescence emission ratio in CD and BCECF due to photo-quenching under 100 watt UV lamp for 3 hours. Reversibility of fluorescence emission ratio due to extreme pH variation in (b) Comparison of pH dependent variation in fluorescence emission from carbon dot and BCECF. (c) carbon dot and (d) BCECF.

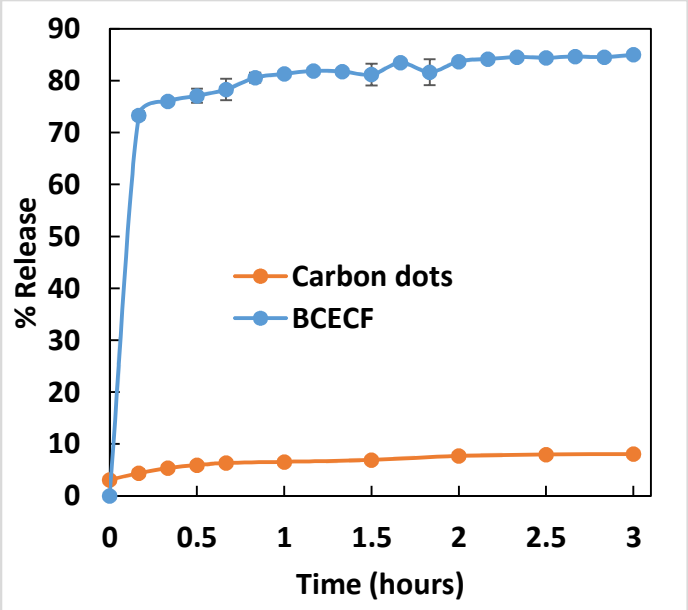

Figure S16. Release profile of carbon dots from microgels in phosphate buffer saline.

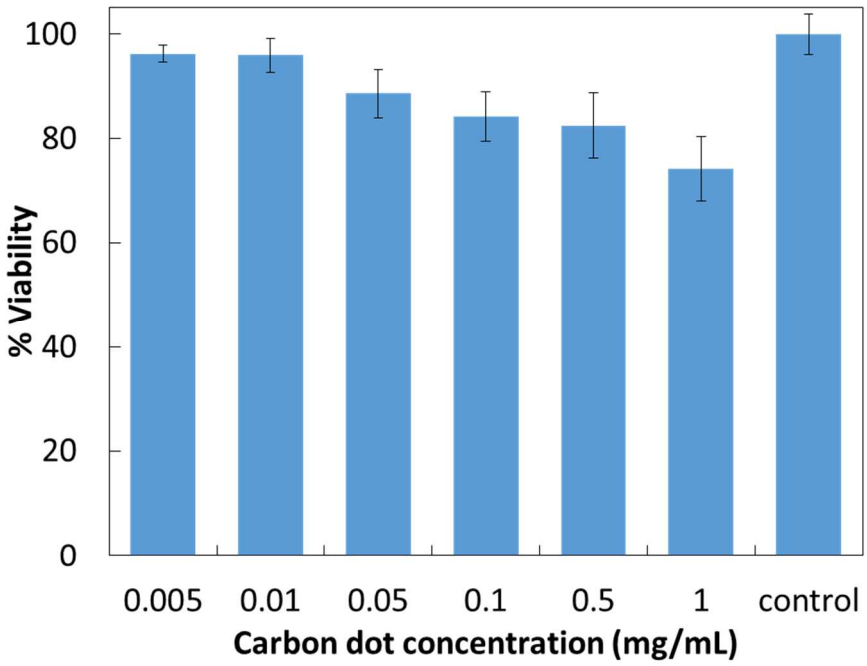

Figure S17. Cytotoxicity of carbon dots as assessed by MTT assay. Viability of more than 80% was observed for carbon dot concentration of 0.5 mg/mL.

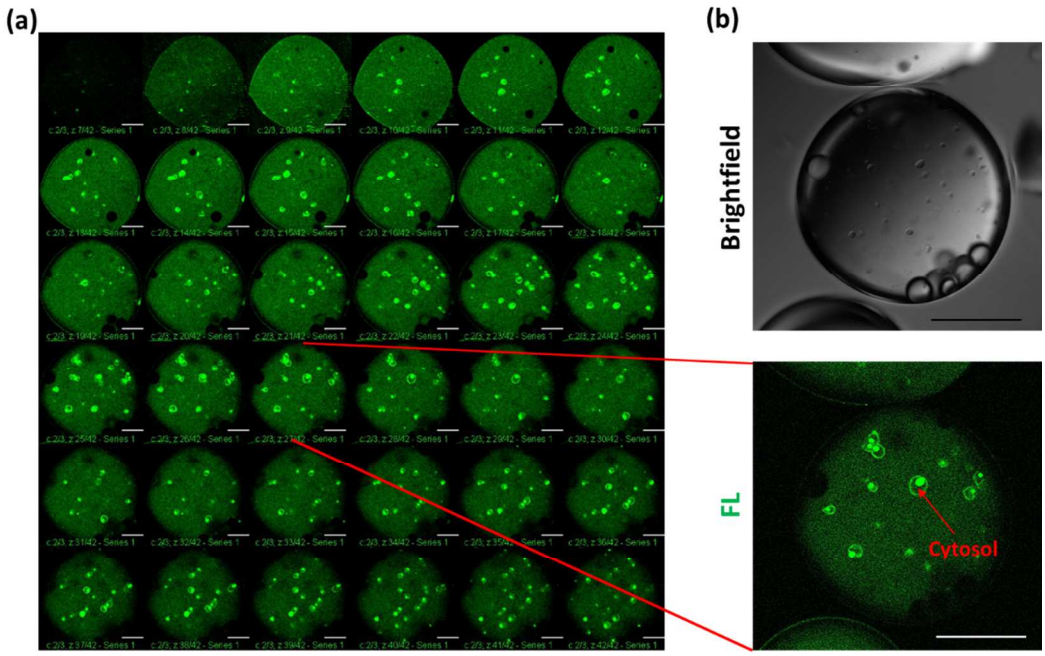

Figure S18. (a) Confocal Z-sectioning fluorescence images of microgel containing cells and carbon dots after 12 days of incubation, showing uniform distribution of carbon dots inside the microgels and its ability to be retained inside the microgels. (Scale bar: 100 µm). (b) Confocal image showing carbon dots around the cells indicated by the non fluorescent cytoplasm. (scale bar: 200 µm).

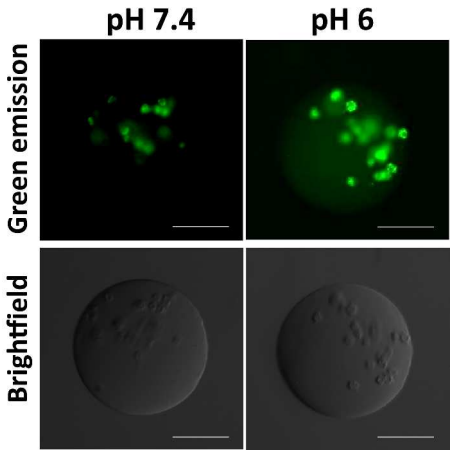

Figure S19. Live cells in the microgel stained by calcein-AM (live cell stain) showing green fluorescence. The microgel at pH 7.4 surrounding has comparatively less fluorescence than the microgels at pH 6, which has more green fluorescence from the microenvironment, as the carbon dots starts fluorescing at pH 6. (Scale bar 100 µm)

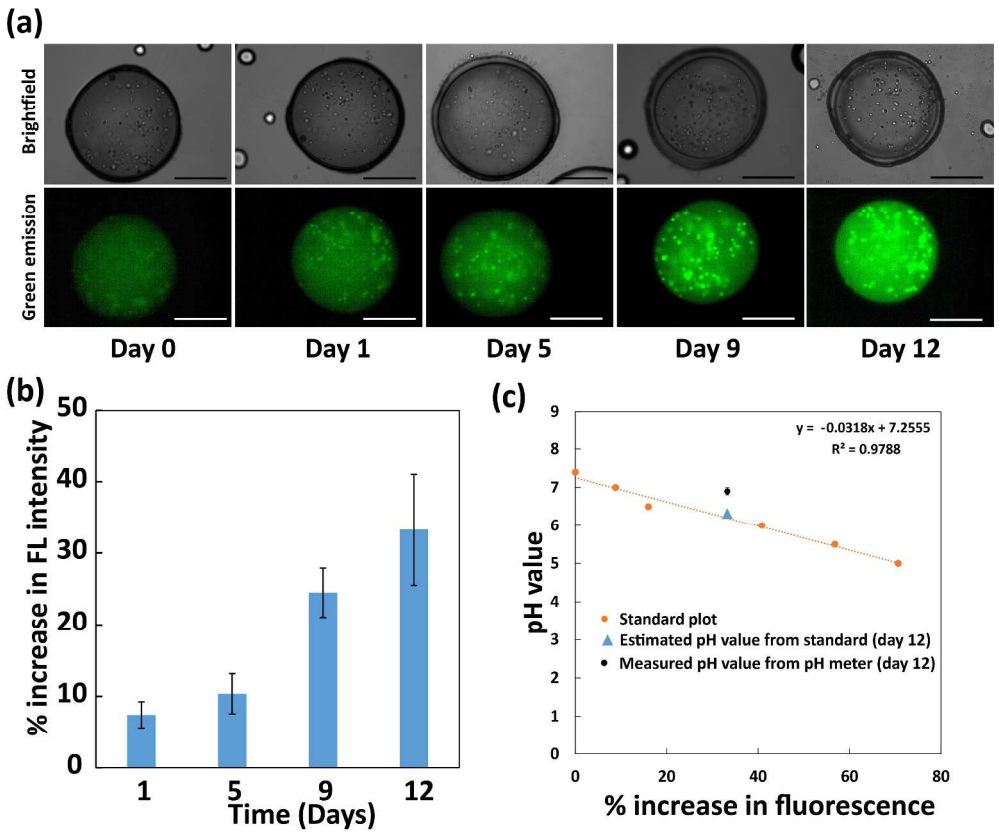

Figure S20. (a) Fluorescence microscopy images of microgels encapsulating HeLa cells placed in paraffin oil over days (scale bar 200 µm). (b) Plot showing normalized fluorescence intensity *vs* time (days) from microgels. The intensity was calculated using images from fluorescence microscopy. (c) Estimated pH values in microgel using % increase in their fluorescence compared to the standard plot. The estimated pH value at day 12 is 6.5 compared to pH 6.9, which is obtained using pH meter.

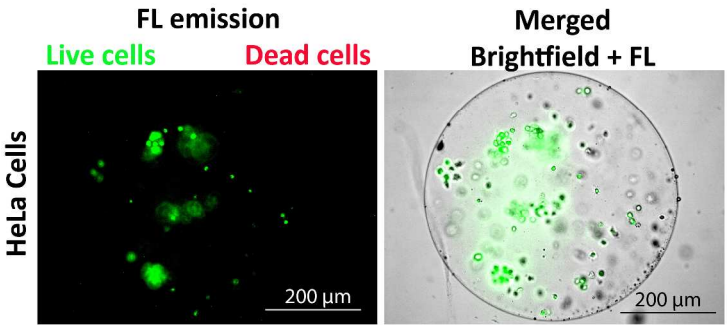

Figure S21: Fluorescence microscopy images showing live and dead assay for HeLa after 12 day incubation of microgel in paraffin oil.

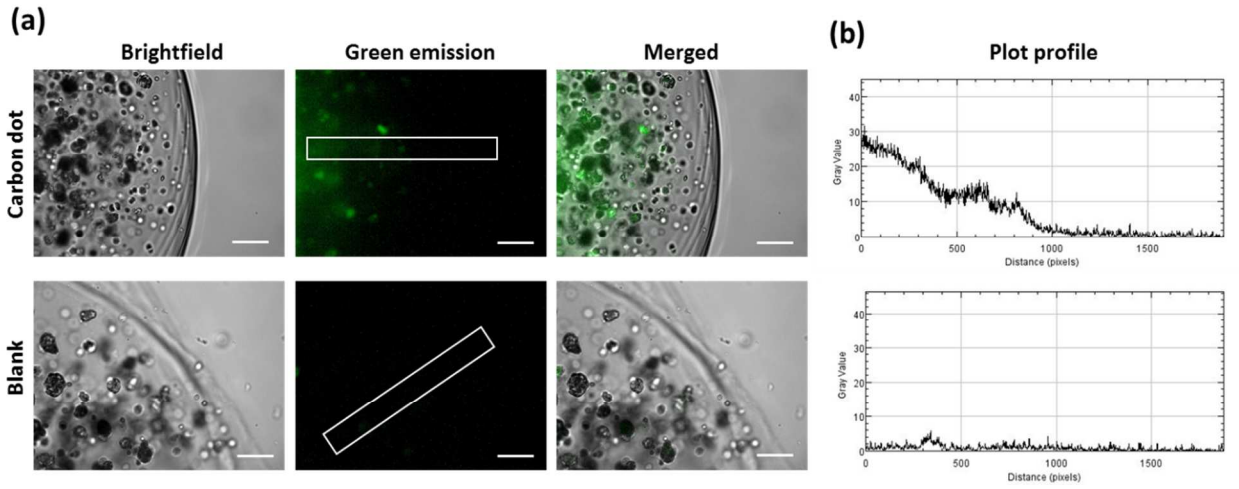

Figure S22. (a) 12 day old Spheroids of MCF-7 Cells cultured in Alginate-RGD hydrogel containing carbon dots show variation in fluorescence emission from periphery towards core. Fluorescence gradient between core and periphery indicates variation in pH. The core is more acidic due comparatively poor diffusion of media and gases, whereas the spheroids in the periphery can easily release molecules outside the microgel. (b) The plot profile showing gradient of fluorescence in microgel containing carbon dots and without them.